



A Lie algebraic theory of barren plateaus for deep parameterized quantum circuits

Received: 11 October 2023

Accepted: 25 June 2024

Published online: 22 August 2024

Check for updates

Michael Ragone^{1,9}, Bojko N. Bakalov^{2,9}, Frédéric Sauvage³, Alexander F. Kemper^{1D}⁴, Carlos Ortiz Marrero^{5,6}, Martín Larocca^{3,7} & M. Cerezo^{1D}⁸✉

Variational quantum computing schemes train a loss function by sending an initial state through a parametrized quantum circuit, and measuring the expectation value of some operator. Despite their promise, the trainability of these algorithms is hindered by barren plateaus (BPs) induced by the expressiveness of the circuit, the entanglement of the input data, the locality of the observable, or the presence of noise. Up to this point, these sources of BPs have been regarded as independent. In this work, we present a general Lie algebraic theory that provides an exact expression for the variance of the loss function of sufficiently deep parametrized quantum circuits, even in the presence of certain noise models. Our results allow us to understand under one framework all aforementioned sources of BPs. This theoretical leap resolves a standing conjecture about a connection between loss concentration and the dimension of the Lie algebra of the circuit's generators.

Variational quantum computing schemes, such as variational quantum algorithms^{1–6} or quantum machine learning models^{7–10}, share a common structure in which quantum and classical resources are used to solve a given task. In a nutshell, these algorithms send some initial state through a parametrized quantum circuit and then perform (a polynomial number of) measurements to estimate the expectation value of some observable that encodes the loss function (also called cost function) appropriate for the problem. Subsequently, the estimated loss (or its gradient) is fed into a classical optimizer that attempts to update the circuit parameters to minimize the loss.

In the past few years, research has started to point towards seemingly fundamental difficulties in training generic parametrized quantum circuits^{11–13}. In particular, one of the main obstacles towards trainability is the presence of Barren Plateaus (BPs)¹³ in the loss function. In the presence of BPs, this loss function (and its gradients) exponentially concentrates in parameter space as the size of the problem increases. Therefore, unless an exponential number of measurement shots are employed, the model becomes untrainable, as one

does not have enough precision to find a loss-minimizing direction and navigate the loss landscape.

Due to the tremendous limitations that BPs place on the potential to scale variational quantum computing schemes to large problem sizes, a significant amount of effort has been put forward towards understanding why and when BPs arise. In this context, the presence of BPs (in the absence of noise) has been shown to arise from several disparate aspects of the variational problem, including the expressiveness of parametrized quantum circuits (that is, the breadth of unitaries that the parametrized quantum circuit can express)^{13–25}, the locality of the loss function measurement operator $O^{26–32}$, and the entanglement and randomness of the initial state $\rho^{13,26,33–37}$. Hardware noise further exacerbates these issues^{38–40}. Yet, despite our significant understanding of BPs, most of the results in the literature have been derived or can be applied only for certain circuit architectures or scenarios. Thus, we cannot generalize the lessons learned from one scenario to another, and the different sources of BPs are regarded as independent. In other words, we do not have a unifying holistic theory

¹Department of Mathematics, University of California Davis, Davis, USA. ²Department of Mathematics, North Carolina State University, Raleigh, USA. ³Theoretical Division, Los Alamos National Laboratory, Los Alamos, USA. ⁴Department of Physics, North Carolina State University, Raleigh, USA. ⁵AI & Data Analytics Division, Pacific Northwest National Laboratory, Richland, USA. ⁶Department of Electrical & Computer Engineering, North Carolina State University, Raleigh, USA. ⁷Center for Nonlinear Studies, Los Alamos National Laboratory, Los Alamos, USA. ⁸Information Sciences, Los Alamos National Laboratory, Los Alamos, USA. ⁹These authors contributed equally: Michael Ragone, Bojko N. Bakalov. ✉ e-mail: cerezo@lanl.gov

that can capture the interplay of the various aspects that give rise to BPs.

In this work, we present a general Lie algebraic theory for BPs that can be applied to any deep, unitary, parametrized quantum circuit architecture. Our theory is based on the study of the Lie group and the associated Lie algebra \mathfrak{g} , which is generated by the parametrized quantum circuit. In turn, this allows us to understand under one single umbrella all known sources of BPs. Critically, we are able to precisely compute the variance of the loss function and, therefore, study its concentration in parameter space, provided that the measured observable O or the circuit's input state ρ is in. Our results encapsulate the known causes of BPs, as we generalize the concepts of circuit expressiveness, initial state entanglement, operator locality, and hardware noise to a unified framework (see Fig. 1). Moreover, we also provide a quantifiable definition for a deep quantum circuit, as we present rigorous bounds for the number of layers needed for it to be an approximate design over the Lie group $e^{\mathfrak{g}}$, and for how much the variances for an exact and for an approximate design deviate.

Results

Loss function and barren plateaus

In what follows, we will consider problems where an n -qubit state ρ , acting on a Hilbert space $\mathcal{H} = (\mathbb{C}^2)^{\otimes n}$, is sent through a parametrized quantum circuit $U(\boldsymbol{\theta})$ of the form

$$U(\boldsymbol{\theta}) = \prod_{l=1}^L e^{iH_l\theta_l}. \quad (1)$$

Here, $\boldsymbol{\theta} = (\theta_1, \theta_2, \dots)$ is a set of trainable real-valued parameters, and $H_l \in i\mathfrak{u}(2^n)$ are Hermitian operators that we collect in a set of generators $\mathcal{G} = \{H_1, H_2, \dots\}$. At the output of the circuit, one measures some Hermitian observable $O \in i\mathfrak{u}(2^n)$, such that $\|O\|_2^2 \leq 2^n$, leading to the loss function,

$$\ell_{\boldsymbol{\theta}}(\rho, O) = \text{Tr}[U(\boldsymbol{\theta})\rho U^\dagger(\boldsymbol{\theta})O]. \quad (2)$$

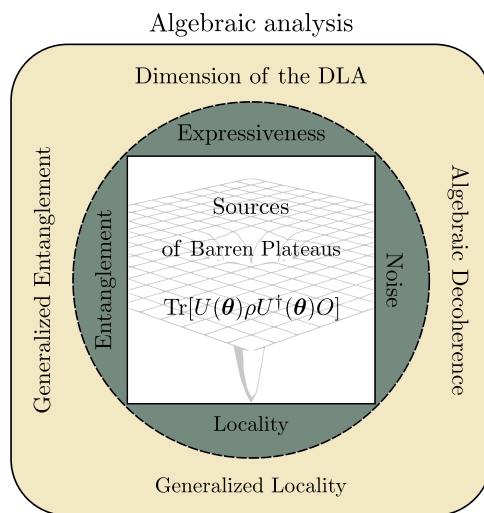


Fig. 1 | Schematic representation of our results. Many works in the literature have shown that BPs can arise from: the expressiveness of the parametrized circuit, the locality of the measurement operator, the entanglement in the initial state, or due to hardware noise. In the figure, we schematically depict these sources as being separate, since their study is usually performed in restricted scenarios, thus limiting our ability to interconnect them. In this work, we present a unified Lie algebraic theory that can be used to study BPs in deep parametrized quantum circuits under SPAM and coherent noise. Our theorems allow us to understand under a single unified framework all sources of BPs by leveraging concepts such as generalized locality entanglement and algebraic decoherence.

Depending on the algorithm at hand, the previous procedure might be repeated for different initial states (e.g., input states coming from some training set), or measurement operators (e.g., measuring different non-commuting observables), and the set of such expectation values can be combined into a more complicated loss function. To account for all of those scenarios, we will simply study a quantity as that in Eq. (2), as we know that if $\ell_{\boldsymbol{\theta}}(\rho, O)$ concentrates, then so will any function computed from it.

Finally, we will consider SPAM errors – which we model by adding completely positive and trace-preserving channels \mathcal{N}_B and \mathcal{N}_A acting before and after the circuit, respectively – and coherent errors, which we represent as uncontrolled unitary gates interleaved with the parametrized gates. When these sources of noise are present, we write the noisy loss function as

$$\tilde{\ell}_{\boldsymbol{\theta}}(\rho, O) = \text{Tr}\left[\mathcal{N}_A\left(\tilde{U}(\boldsymbol{\theta})\mathcal{N}_B(\rho)\tilde{U}^\dagger(\boldsymbol{\theta})\right)O\right], \quad (3)$$

where $\tilde{U}(\boldsymbol{\theta}) = \prod_{l=1}^L e^{-i\alpha_l K_l} e^{iH_l\theta_l}$ for fixed (not tunable) real values α_l and Hermitian operators K_l .

In what follows, we will study how much the loss $\ell_{\boldsymbol{\theta}}(\rho, O)$ (or its noisy counterpart $\tilde{\ell}_{\boldsymbol{\theta}}(\rho, O)$) changes as the parameters $\boldsymbol{\theta}$ vary. In particular, we want to characterize the variance of the loss over the parameter landscape,

$$\text{Var}_{\boldsymbol{\theta}}[\ell_{\boldsymbol{\theta}}(\rho, O)] = \mathbb{E}_{\boldsymbol{\theta}}[\ell_{\boldsymbol{\theta}}(\rho, O)^2] - (\mathbb{E}_{\boldsymbol{\theta}}[\ell_{\boldsymbol{\theta}}(\rho, O)])^2, \quad (4)$$

and we will say that the loss exhibits a BP if the variance vanishes exponentially with the system size, i.e., if $\text{Var}_{\boldsymbol{\theta}}[\ell_{\boldsymbol{\theta}}(\rho, O)] \in \mathcal{O}(1/b^n)$, for some $b > 1$. It is important to note that in the literature it is common to study the presence of BPs by analyzing the concentration of the partial derivatives of the loss, i.e., the scaling of $\text{Var}_{\boldsymbol{\theta}}[\frac{\partial \ell_{\boldsymbol{\theta}}(\rho, O)}{\partial \theta_\mu}]$. However, since loss concentration implies partial derivative concentration⁴¹, in what follows we exclusively focus on the former. Moreover, our results on the variance of the loss function can be modified in a straightforward way to obtain the variance of the partial derivatives.

Dynamical Lie algebra

Computing the variance of the loss function requires evaluating averages over the parameter landscape. When the circuit is sufficiently deep, we can leverage Lie algebraic tools to perform such calculations. To this end, we define the so-called dynamical Lie algebra (DLA)^{42–44} of the parametrized quantum circuit (we will assume a circuit with no coherent errors for the remainder of this section). The DLA is defined as the Lie closure of the circuit's generators,

$$\mathfrak{g} = \langle i\mathcal{G} \rangle_{\text{Lie}}, \quad (5)$$

which is the (closed under commutation) subspace of $i\mathfrak{u}(2^n)$ spanned by the nested commutators of the generators $i\mathcal{G}$. Since \mathfrak{g} is a subalgebra of the Lie algebra $i\mathfrak{u}(2^n)$ of skew-Hermitian operators acting on \mathcal{H} , it is a reductive Lie algebra (see, e.g., ref. 45, Chapter IV). This means that we can express \mathfrak{g} as a direct sum of commuting ideals,

$$\mathfrak{g} = \mathfrak{g}_1 \oplus \cdots \oplus \mathfrak{g}_{k-1} \oplus \mathfrak{g}_k, \quad (6)$$

where \mathfrak{g}_j are simple Lie algebras for $j = 1, \dots, k-1$ and \mathfrak{g}_k is abelian (so \mathfrak{g}_k is the center of \mathfrak{g} and $[\mathfrak{g}, \mathfrak{g}] = \mathfrak{g}_1 \oplus \cdots \oplus \mathfrak{g}_{k-1}$ is semisimple). In the Methods we provide additional intuition as to why the DLA takes the form in Eq. (6). The importance of the DLA comes from the fact that it quantifies the ultimate expressiveness of the parametrized quantum circuit: we have $U(\boldsymbol{\theta}) \in G = e^{\mathfrak{g}}$ for all $\boldsymbol{\theta}$.

In the following, we assume that the parametrized circuit is deep enough so that it forms a 2-design on each of the simple or abelian components $G_j = e^{\mathfrak{g}_j}$ ($j = 1, \dots, k$) (i.e., the first two moments of the

distribution of unitaries obtained from the circuits, match those of the Haar measure over each group G_j ⁴⁶, which will allow us to compute the variance via an explicit integration over the Lie group. Our results are readily useful to analyze the variance of circuits that form approximate, rather than exact, designs. In particular, in the Methods and the Supplemental Information, we present and prove Theorems 2 and 3, which respectively set bounds on the necessary number of layers for the circuit to become an ϵ -approximate 2-design over G , and bound the difference between the variance of a 2-design circuit and that of an L -layered circuit that does not necessarily form a 2-design over G . Then, for any function $f(U(\theta))$ that is a polynomial of order (up to) two in the matrix elements of $U(\theta)$ and its conjugate transpose, we will compute averages over the parameter landscape as $\mathbb{E}_\theta[f(U(\theta))] = \prod_{j=1}^k \int_{G_j} d\mu_j f(U(\theta))$, where $d\mu_j$ is the normalized, left- and right-invariant Haar measure on G_j . Such integrals can be evaluated using Weingarten Calculus (see, e.g.,⁴⁷), and we present a simple approach based on the invariant theory of Lie algebras.

Finally, our results use a generalized notion of purity with respect to an arbitrary operator subalgebra $\mathfrak{g} \subseteq \mathfrak{u}(2^n)$. The \mathfrak{g} -purity of a Hermitian operator $H \in i\mathfrak{u}(2^n)$ is defined as^{48,49}

$$\mathcal{P}_{\mathfrak{g}}(H) = \text{Tr}[H_{\mathfrak{g}}^2] = \sum_{j=1}^{\dim(\mathfrak{g})} \left| \text{Tr}[B_j^\dagger H] \right|^2, \quad (7)$$

where $H_{\mathfrak{g}}$ denotes the orthogonal projection of H into $\mathfrak{g}_{\mathbb{C}} = \text{span}_{\mathbb{C}} \mathfrak{g}$ (the complexification of \mathfrak{g}) and $\{B_j\}_{j=1}^{\dim(\mathfrak{g})}$ an orthonormal basis (over \mathbb{C}) for $\mathfrak{g}_{\mathbb{C}}$ with respect to the Hilbert–Schmidt inner product $\langle A, B \rangle = \text{Tr}[A^\dagger B]$ ⁴⁵. Note that $H_{\mathfrak{g}} \in i\mathfrak{g}$ and the basis vectors B_j are chosen from $i\mathfrak{g}$; in that case, $\text{Tr}[B_j^\dagger H] = \text{Tr}[B_j H] \in \mathbb{R}$. In the Supplemental Information, we provide some intuition about why the \mathfrak{g} -purity arises as the natural quantity in our results.

Main result

In this section, we present an exact formula for the variance of the loss function. To simplify the presentation, we will first restrict ourselves to noiseless circuits and incorporate noise as we proceed. Our main theorem exploits the reductiveness of the DLA: when either $\rho \in i\mathfrak{g}$ or $O \in i\mathfrak{g}$, the loss (and its variance) can be expanded into individual terms arising from each ideal $\mathfrak{g}_j \subseteq \mathfrak{g}$ (see the “Methods” and Supplemental Information for additional details). Equipped with this result, we can prove the following theorem:

Theorem 1. Suppose that $O \in i\mathfrak{g}$ or $\rho \in i\mathfrak{g}$, where the DLA \mathfrak{g} is as in Eq. (6). Then the mean of the loss function vanishes for the semisimple component $\mathfrak{g}_1 \oplus \dots \oplus \mathfrak{g}_{k-1}$ and leaves only abelian contributions:

$$\mathbb{E}_\theta[\ell_\theta(\rho, O)] = \text{Tr}[\rho_{\mathfrak{g}_k} O_{\mathfrak{g}_k}]. \quad (8)$$

Conversely, the variance of the loss function vanishes for the center \mathfrak{g}_k and leaves only simple contributions:

$$\text{Var}_\theta[\ell_\theta(\rho, O)] = \sum_{j=1}^{k-1} \frac{\mathcal{P}_{\mathfrak{g}_j}(\rho) \mathcal{P}_{\mathfrak{g}_j}(O)}{\dim(\mathfrak{g}_j)}. \quad (9)$$

Let us now consider the implications of Theorem 1. As we can see from Eq. (8), the mean of the loss is solely determined by the projections of ρ and O onto the center \mathfrak{g}_k of \mathfrak{g} . As such, if \mathfrak{g} is centerless, then $\mathbb{E}_\theta[\ell_\theta(\rho, O)] = 0$. Conversely, if \mathfrak{g} is abelian and if ρ or O commutes with \mathfrak{g} (a slightly more general condition than belonging to \mathfrak{g}), then the loss landscape is completely flat.

Next, we turn our attention to Eq. (9). This equation shows that each term in the variance of the loss function depends on three quantities: the dimension of \mathfrak{g}_j , and the \mathfrak{g}_j -purities of ρ and O . To understand what each of these terms means, let us focus on the case

where \mathfrak{g} is simple. Then Eq. (9) has a single term,

$$\text{Var}_\theta[\ell_\theta(\rho, O)] = \frac{\mathcal{P}_{\mathfrak{g}}(\rho) \mathcal{P}_{\mathfrak{g}}(O)}{\dim(\mathfrak{g})}. \quad (10)$$

The following result, proved in the Supplemental Information, illustrates the fact that BPs can arise from three sources.

Corollary 1. Let $\|O\|_2^2 \leq 2^n$. If either $\dim(\mathfrak{g})$, $1/\mathcal{P}_{\mathfrak{g}}(\rho)$ or $1/\mathcal{P}_{\mathfrak{g}}(O)$ is in $\Omega(b^n)$ with $b > 2$, then the loss has a BP.

In what follows, we analyze these three causes of BPs.

Sources of barren plateaus

(i) Ansatz expressiveness and the DLA. First, we observe from Theorem 1 that the variance is inversely proportional to $\dim(\mathfrak{g})$, which directly quantifies the expressiveness of the circuit; that is, more expressive circuits (with larger $\dim(\mathfrak{g})$) lead to more concentrated loss functions (see Fig. 2a). In particular, as shown in Corollary 1, if the dimension of the DLA is in $\Omega(b^n)$ for some $b > 2$, then the loss is exponentially concentrated regardless of the initial state or measurement operator. Thus, deep circuits with exponential DLAs are always untrainable. On the other hand, if $\dim(\mathfrak{g}) \in \mathcal{O}(\text{poly}(n))$ (see examples of polynomially scaling DLAs in refs. 50–53), the expressiveness of the circuit will not induce BPs by itself. As we will see below, this does not preclude the possibility that the initial state or the measurement operator could still lead to exponential concentration. Importantly, this result proves (under the assumption that ρ or O is in $i\mathfrak{g}$) the conjecture proposed in ref. 17, where the authors argue precisely that the loss variance should be inversely proportional to the expressive power of the circuit, captured by the DLA dimension.

(ii) Initial quantum state ρ . Second, we consider the \mathfrak{g} -purity of a quantum state, $\mathcal{P}_{\mathfrak{g}}(\rho) = \text{Tr}[\rho_{\mathfrak{g}}^2]$. This quantity has been studied in the literature and is known to be a measure of generalized entanglement^{54,55}. As discussed in ref. 55, one can define a generalization of entanglement relative to a subspace of observables rather than the usual approach, where distinguished subsystems are used to define the entanglement. In standard entanglement theory, the preferred subspaces of observables are given by the local operators that act only on each subsystem, and a pure entangled state looks mixed when partially tracing over one of the subsystems (producing a reduced state). This notion can be generalized by imposing that reduced states of a quantum system only provide the expectations of some set of distinguished observables, and we say that a state is generalized unentangled relative to the distinguished observables if its reduced state is pure (cf. Fig. 2b). Taking the subspace of observables to be the DLA leads precisely to this generalized measure of entanglement. In this framework, the purity $\mathcal{P}_{\mathfrak{g}}(\rho)$ is maximized (ρ is not generalized entangled) if ρ belongs to the orbit of the highest weight state of \mathfrak{g} (see Methods for a definition of the highest weight state, as well as a particular case where we specialize to ρ or O simultaneously diagonalizable with a Cartan subalgebra $\mathfrak{h} \subseteq \mathfrak{g}$). Essentially, a smaller \mathfrak{g} -purity implies larger generalized entanglement and, in turn, smaller variances. Hence, if $\mathcal{P}_{\mathfrak{g}}(\rho) \in \mathcal{O}(1/b^n)$ (high generalized entangled state), the loss concentrates exponentially regardless of the circuit expressiveness, that is, even if $\dim(\mathfrak{g})$ is polynomial.

(iii) Measurement operator O . Finally, we turn to the \mathfrak{g} -purity of the measurement operator O (cf. Fig. 2c). We carry over the notion of generalized entanglement to define a generalized notion of locality: We call an operator O generalized-local if it belongs to the preferred subspace of observables given by \mathfrak{g} . In this case, $O_{\mathfrak{g}} = O$. On the other hand, we will call it (fully) generalized nonlocal if $O_{\mathfrak{g}} = 0$. This definition allows us to establish a hierarchy of locality when O belongs to the DLA’s associative algebra (the matrix-product closure of \mathfrak{g}). Here, one can classify the amount of generalized locality by expressing O as a polynomial of elements of \mathfrak{g} , and filter them according to the

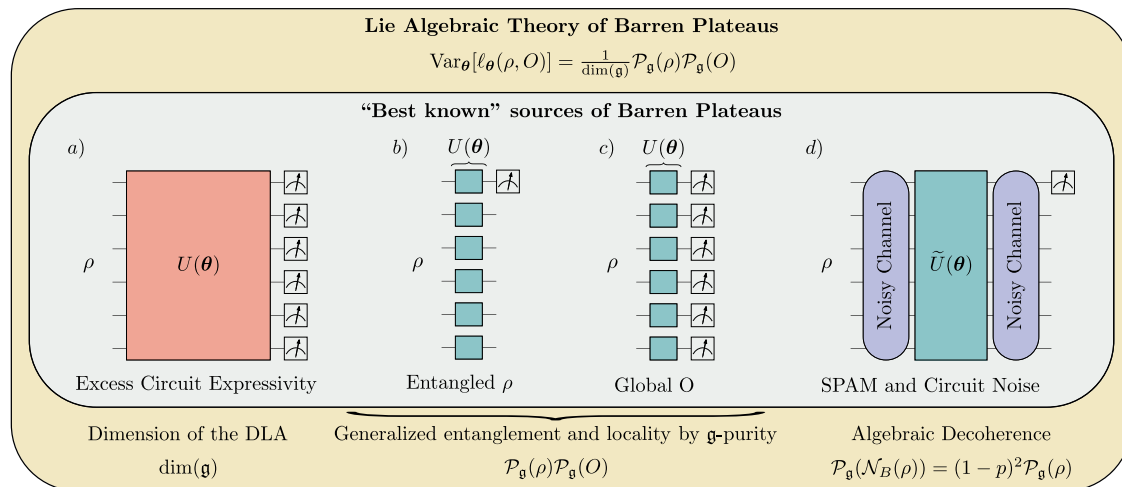


Fig. 2 | Source of barren plateaus under our framework. The “best known” sources of BPs include: (a) circuits that are too expressive with $\dim(g) \sim 4^n$, for any O, ρ ; (b) highly entangled initial states ρ , even for shallow circuits and local O ; (c) global operators O , even for shallow circuits; (d) noise channels. Our framework

unifies these sources in one holistic picture, characterizing the circuit expressivity as $\dim(g)$, the initial state and operator properties by generalized entanglement and locality via g -purity, and noise channels by algebraic decoherence.

polynomial’s degree; more local operators will be those that can be expressed as polynomials of lower degree. With the above definition, one can readily see that generalized local operators (i.e., those satisfying $O_g = O$) maximize the variance. On the other hand, when $O_g \in \mathcal{O}(1/b^n)$ (highly generalized nonlocal measurements), the loss exhibits a BP regardless of the DLA dimension.

Putting points (i)–(iii) together, our results in Theorem 1 imply that the loss concentration is completely determined by the expressiveness of the parametrized quantum circuit, the generalized entanglement of the input state, and the generalized locality of the measurement operator. When the DLA g is not simple, in order for the loss to be exponentially concentrated and a BP to occur, each of the components g_j needs exponentially large DLAs, highly generalized-entangled states, or very generalized-nonlocal measurements. When this condition is not satisfied on some of the components g_j , one can train the loss function only on the signal from these components, but only for those particular components g_j ; for the remainder, the variances are exponentially suppressed.

Incorporating the effects of noise

To finish, we consider how SPAM noise and coherent errors affect the variance scaling (cf. Fig. 2d). We begin by considering the case of state preparation noise, assuming $O \in ig$. The effect of noise is to change the initial state from ρ to $\mathcal{N}_B(\rho)$. From Theorem 1, we find that if the g -purity of the state decreases (in some or all components g_j of g), then so will the variance. This will be the case for global depolarizing noise $\mathcal{N}_B(\rho) = (1-p)\rho + p\mathbb{1}/2^n$, which takes $\mathcal{P}_g(\rho)$ to $\mathcal{P}_g(\mathcal{N}_B(\rho)) = (1-p)^2 \mathcal{P}_g(\rho)$. Moreover, we can see that even local unitaries acting on a single qubit during state preparation (which would preserve the standard purity $\text{Tr}[\rho^2]$ of the state and the standard entanglement) can lead to a generalized-entanglement-induced loss concentration if they rotate the state outside of ig . These examples showcase a form of algebraic decoherence, whereby the state gets entangled with either an actual environment (e.g., the previous case of depolarizing noise) or with an effective “algebraic environment” within the system.

Next, we consider the presence of measurement errors. We can model this with a channel \mathcal{N}_A^{-1} acting on O , where \mathcal{N}_A^{-1} denotes the inverse of the noise channel \mathcal{N}_A , which is generally not a physical quantum channel. In this case, if the g -purity of the measurement operator decreases, i.e., if O loses generalized locality, then the loss concentrates.

Finally, we study the effect of coherent errors that occur during circuit execution. In this case, we can model their impact as uncontrolled unitaries acting along the circuit, which will change the set of generators to $\tilde{\mathcal{G}} = \mathcal{G} \cup \{iK_I\}$, and thus the DLA becomes $\tilde{g} \supseteq g$. Interestingly, this means that coherent noise can increase the expressiveness of the circuit at the cost of potentially decreasing the variance. To know exactly how the variance changes, one needs to study the reductive decomposition of \tilde{g} , as well as the \tilde{g} -purities of ρ and O in this new noise-induced DLA.

Discussion

Finding ways to avoid or mitigate barren plateaus (BPs) has been one of the central topics of research in variational quantum computing. This has led the community to develop a series of good practice guidelines such as: “global observables where one measures all qubits are untrainable” or “too much entanglement leads to BPs.” While these are widely regarded as being universally true, they are in fact obtained by extrapolating results derived for a specific circuit architecture and assuming that they will hold in another. Many of these misconceptions are propagated due to a lack of a single unifying theory of BPs that truly connects the results obtained for different architectures. In this work, we present one such theory based on the Lie algebraic properties of the parametrized quantum circuit, the initial state, and the measurement operator.

Despite the relative simplicity of our main theorem, its implications are extremely important to the field of variational quantum computing. First, it is worth highlighting that, unlike other results, our theorems provide exact variance calculations rather than upper or lower bounds, thus allowing us to precisely determine whether we will or will not have a BP. Second, we note that our theorem applies to any (noiseless) deep parametrized quantum circuit, independent of its structure, but requiring only knowledge of the DLA of the circuit (and provided that ρ or O are in ig). This makes our results applicable in essentially all areas of variational quantum computing. Conceptually, our results uncover the precise role that entanglement and locality play in the nature of BPs. However, they do so by being defined in terms of the operators in the DLA rather than in terms of local operators determined by the qubit-subsystem decomposition. As such, it is entirely possible for a circuit to be trained on highly entangled initial states using highly nonlocal measurements (i.e., acting on all qubits) as long as they are well aligned with the underlying DLA of the circuit. This goes against one of the best practices in the field and

demonstrates that a more subtle approach is valuable. It is also worth noting that our algebraic formalism allows us to consider simple noise models such as SPAM errors and coherent noise. Our analysis shows that noise-induced concentration can be understood as building generalized entanglement in the initial state, reducing the generalized locality of the measurement observable, or increasing the expressive power of the circuit.

Looking ahead, we see different ways to extend our results. For example, our theorems are derived for the case where ρ or O is in $i\mathfrak{g}$. Although this case encompasses most algorithms in the literature^{1–3}, it could be interesting to generalize our results to operators and measurements not in the DLA. We refer the readers to ref. 56, where exact loss function variance calculations are presented for a parametrized matchgate circuit, which is valid for arbitrary measurements and initial states. We hope that the results therein will serve as a blueprint for a general theory for generic circuits. Moreover, one can also envision considering more realistic noise settings where noise channels are interleaved with the unitaries. Clearly, since a noisy parametrized quantum circuit no longer forms a group, our Lie algebraic formalism no longer applies. Similarly, we encourage the community to develop tools to compute the exact variance for circuits that do not form approximate 2-designs, as these cases are not covered by our main theorems. In this case, a Lie algebraic treatment such as the one presented here will not be available. Here, one will have to instead make additional assumptions such as local gates being sampled from a local group, thus mapping the variance evaluation to a Markov chain-like process which can be analyzed analytically^{21,26,27,57–64}, numerically via Monte Carlo⁶⁵ and tensor networks^{66,67}, or studied via XZ-calculus⁶⁸. Moreover, we note that recent results have tied the DLA and the presence or absence of barren plateaus to other phenomena like the simulability of the quantum model^{56,69}, to the presence of local minima in the optimization landscape⁷⁰, and to the reachability of solutions (through the disconnectedness in the geometric manifold of unitaries⁷¹). We expect that in the near future, the generalized notions of entanglement and locality discussed here will be connected to the resources needed to make a model more or less universal, more or less simulable, and more or less trainable. Such connections will shed additional light on the central role that the DLA plays in characterizing variational quantum computing models.

Note added. A few days before our work was submitted to the arXiv, the manuscript⁷² was posted as a preprint. In ref. 72, the authors provide an independent proof of the conjecture in¹⁷ and present results similar to those in our theorems and examples. However, we note that in Ref. 72 the authors study partial derivative concentration rather than loss concentration as we do. Moreover, our work provides a novel conceptual understanding of the variance \mathfrak{g} -purity terms as forms of generalized entanglement and locality. As such, our work complements that of⁷², and we encourage the reader to review both manuscripts.

Methods

In this section, we first recall a few basic concepts for the DLA, present examples that showcase how our results can be used to understand several BP results in the literature (see Fig. 2) and derive additional theorems that justify some of the assumptions made in the main text. We also present concrete examples where we can analytically compute the \mathfrak{g} -purities of the state and the measurement operator. Furthermore, in the Supplemental Information, we include numerical simulations that illustrate our theoretical findings.

Symmetries and the DLA structure

In Eq. (6) we have argued that the DLA can be generically decomposed as a direct sum of commuting ideals. Here we provide additional intuition as to why this is the case. First, let us begin by denoting as $\text{comm}(\mathcal{G})$ the commutant of the set of generators \mathcal{G} (i.e., the

symmetries of the gate generators), that is,

$$\text{comm}(\mathcal{G}) = \{A \in \mathbb{C}^{2^n \times 2^n} \mid [A, H] = 0 \forall H \in \mathcal{G}\}, \quad (11)$$

and as \mathfrak{z} the center of $\text{comm}(\mathcal{G})$, i.e.,

$$\mathfrak{z} = \{B \in \text{comm}(\mathcal{G}) \mid [B, L] = 0 \forall L \in \text{comm}(\mathcal{G})\}. \quad (12)$$

The importance of the commutant $\text{comm}(\mathcal{G})$ and its center \mathfrak{z} span from the fact that they determine the invariant subspaces of the Hilbert space under the action of $G = e^{\mathfrak{g}}$. Moreover, the dimension of the center is directly related to the DLA's decomposition as we can rewrite the decomposition of \mathfrak{g} into commuting ideals as

$$\mathfrak{g} = \bigoplus_{\lambda=1}^{\dim(\mathfrak{z})} \mathbb{1}_{m_\lambda} \otimes \mathfrak{g}_\lambda, \quad (13)$$

with m_λ denoting the multiplicity of the representation \mathfrak{g}_λ of \mathfrak{g} . We may interpret such a direct sum decomposition as saying, “There exists a basis of our Hilbert space that block-diagonalizes the matrices in \mathfrak{g} .”

Equation (13) shows that a circuit with symmetries will have a rich and complex DLA structure, while universal, unstructured circuits will likely lead to controllable circuits with $\mathfrak{g} = \mathfrak{su}(2^n)$. In particular, we note that while there have been significant recent efforts on computing DLAs^{44,50–53,71,73}, this field is still in its infancy, and we predict that as our understanding and ability to calculate the DLA increases, the results of the present work will become more and more important for studying the trainability of structured parametrized quantum circuits.

Examples of barren plateaus and their origins

In this section, we review some results in the literature that have studied different sources of BPs, and we show how these results can be understood by our framework.

(i) Expressiveness. One of the most studied sources of BPs is the expressiveness of the circuit^{13–25}. As previously noted, by expressiveness we mean the breadth of unitaries that the circuit can generate as the parameters are varied.

For example, let us consider the case where the unitary $U(\boldsymbol{\theta})$ forms a 2-design⁴⁶ over $\mathbb{SU}(2^n)$ (see Fig. 2a). This is precisely the case studied in the seminal work of Ref. 13. Here, $\mathfrak{g} = \mathfrak{su}(2^n)$, meaning that $\dim(\mathfrak{g}) = 4^n - 1$. From Theorem 1, we find $\mathbb{E}_{\boldsymbol{\theta}}[\ell_{\boldsymbol{\theta}}(\rho, O)] = 0$ (because the Lie algebra has no center), and

$$\begin{aligned} \text{Var}_{\boldsymbol{\theta}}[\ell_{\boldsymbol{\theta}}(\rho, O)] &= \frac{1}{4^n - 1} \text{Tr}[O_{\mathfrak{g}}^2] \text{Tr}[\rho_{\mathfrak{g}}^2] \\ &= \frac{1}{4^n - 1} \left(\text{Tr}[O^2] - \frac{\text{Tr}[O]^2}{2^n} \right) \left(\text{Tr}[\rho^2] - \frac{1}{2^n} \right). \end{aligned} \quad (14)$$

In the second line above, we have used the fact that, because $i\mathfrak{su}(2^n)$ contains all Pauli matrices except the identity $\mathbb{1}$, we have $O_{\mathfrak{g}} = O - 2^{-n} \text{Tr}[O] \mathbb{1}$ and similarly for ρ (which has $\text{Tr}[\rho] = 1$). Since $\text{Tr}[O^2] \leq 2^n$ (by assumption) and noting that $\text{Tr}[\rho^2] - 2^{-n} \leq 1$, we find that $\text{Var}_{\boldsymbol{\theta}}[\ell_{\boldsymbol{\theta}}(\rho, O)] \in \mathcal{O}(1/2^n)$. Hence, we can see that, regardless of what O and ρ are, the expressiveness of the circuit will always lead to a BP.

(ii) Measurement locality. A second potential source of BPs is the measurement operator^{26–32}. For example, consider the task of sending $\rho = |O\rangle\langle O|^{\otimes n}$ through a circuit $U(\boldsymbol{\theta})$ composed of general single-qubit gates. Clearly, this parametrized quantum circuit is very inexpensive as it does not generate entanglement; in fact, we can easily find that $\mathfrak{g} = \mathfrak{su}(2)^{\oplus n}$. As shown in ref. 26, if the measurement is global (see Fig. 2c), e.g., $O = X^{\otimes n}$, one has a BP since $\text{Var}_{\boldsymbol{\theta}}[\ell_{\boldsymbol{\theta}}(\rho, O)] \in \mathcal{O}(1/2^n)$. However, measuring an operator in \mathfrak{g} , such as $O = X_1$ (see Fig. 2c), does

not lead to BPs. Now Theorem 1 indicates that $\mathbb{E}_{\theta}[\ell_{\theta}(\rho, O)] = 0$ and

$$\begin{aligned}\text{Var}_{\theta}[\ell_{\theta}(\rho, O)] &= \sum_{j=1}^n \frac{1}{3} \text{Tr}[O_{g_j}] \text{Tr}[\rho_{g_j}^2] \\ &= \frac{1}{3} \text{Tr}[O_{g_1}^2] \text{Tr}[\rho_{g_1}^2] = \frac{1}{3} \\ &= \frac{1}{3} \text{Tr}_{\mathbb{C}^2}[O_1^2] \left(\text{Tr}_{\mathbb{C}^2}[\rho_1^2] - \frac{1}{2} \right),\end{aligned}\quad (15)$$

where $\text{Tr}_{\mathbb{C}^2}$ denotes the trace over the qubit where O acts. Indeed, we have $\mathfrak{g} = \mathfrak{g}_1 \oplus \dots \oplus \mathfrak{g}_n$ with each $\mathfrak{g}_j \cong \mathfrak{su}(2)$. Using the orthonormal basis $\{2^{-n/2}X_j, 2^{-n/2}Y_j, 2^{-n/2}Z_j\}$ of $i\mathfrak{g}_j$, we find $O_{g_1} = X_1$ and $O_{g_j} = 0$ for $2 \leq j \leq n$, while $\rho_{g_j} = 2^{-n}Z_j$ for all j . This gives $\text{Tr}[O_{g_1}^2] = 2^n$, $\text{Tr}[\rho_{g_1}^2] = 2^{-n}$, yielding the value 1/3 on the second line of Eq. (15). The last line in Eq. (15) provides an alternative interpretation, where the observable O and state ρ are reduced on the first qubit to $O_1 = X$ and $\rho_1 = |0\rangle\langle 0|$, respectively. Note that the last line in Eq. (15) is the special case $n=1$ of Eq. (14). Thus, in this specific case, the notions of generalized entanglement and generalized locality match their standard notions based on the subsystem decomposition of the Hilbert space. As such, if we measure a local operator in qubit j , the variance will depend on the purity of the reduced (input) state over qubit j .

(iii) Initial state entanglement. Next, it has been shown that initial state entanglement can lead to BPs^{13,26,33–37}. For instance, consider again the circuit in Fig. 2c, where $U(\theta)$ is composed of single qubit gates, and let the measurement operator be local, e.g., $O = X_1$. Although we do not expect expressiveness- or locality-induced BPs, if the initial state ρ satisfies a volume law of entanglement (i.e., if the reduced state on any qubit is exponentially close to being maximally mixed), then $\text{Tr}_{\mathbb{C}^2}[\rho_1^2] \in O(1/2^n)$ and the loss has a BP according to Eq. (15).

(iv) Noise. Finally, the presence of hardware noise has been shown to induce loss function concentration^{38–40}. As an example, consider the circuit in Fig. 2d, where a global depolarizing noise channel $\mathcal{N}_B(\rho) = (1-p)\rho + p2^{-n}\mathbb{I}$ acts at the beginning of the circuit (e.g., as part of the SPAM errors). Now, we have $\tilde{\ell}_{\theta}(\rho, O) = (1-p)\ell_{\theta}(\rho, O) + p2^{-n}\text{Tr}[O]$. As p increases, we can see that $\text{Var}_{\theta}[\tilde{\ell}_{\theta}(\rho, O)] = (1-p)^2\text{Var}_{\theta}[\ell_{\theta}(\rho, O)]$ approaches 0 and the loss concentrates around $2^{-n}\text{Tr}[O]$.

Deep parametrized quantum circuits form 2-designs

Let us here show that if the circuit is deep enough, then it will form a 2-design on each of the simple or abelian components of the DLA. In particular, we answer the question: How many layers are needed for $U(\theta)$ to become an approximate 2-design over G ?

First, let us express the parametrized quantum circuit by factorizing it into layers. That is, we take $U(\theta) = U_L(\theta_L)U_{L-1}(\theta_{L-1}) \dots U_1(\theta_1)$ where each layer $U_i(\theta_i)$ is given by $U_i(\theta_i) = \prod_{k=1}^K e^{-iH_k\theta_{ik}}$. Next, let us denote the ensemble of unitaries generated by the L -layered circuit $U(\theta)$ by \mathcal{E}_L , and its t -th moment operator $\mathcal{M}_{\mathcal{E}_L}^{(t)} : \mathfrak{gl}(\mathcal{H}^{\otimes t}) \rightarrow \mathfrak{gl}(\mathcal{H}^{\otimes t})$ is the linear superoperator given by

$$\mathcal{M}_{\mathcal{E}_L}^{(t)}(\cdot) = \int_{\mathcal{E}_L} d\mu(U) U^{\otimes t} (\cdot) (U^{\dagger})^{\otimes t}. \quad (16)$$

The importance of $\mathcal{M}_{\mathcal{E}_L}^{(t)}$ arises from the fact that it allows us to compare how expressive, or how close, a given $U(\theta)$ is to the Haar ensemble over G . In particular, denoting as $\mathcal{M}_G^{(t)}$ the moment operator for the Haar ensemble over G , one can quantify the expressiveness of the circuit via the norm of the superoperator,

$$\mathcal{A}_{\mathcal{E}_L}^{(t)} = \mathcal{M}_{\mathcal{E}_L}^{(t)} - \mathcal{M}_G^{(t)}. \quad (17)$$

For our purposes, we work with the Schatten p -norms where $p=1, \infty$ on the spaces of operators $\mathfrak{gl}(\mathcal{H}^{\otimes t})$. Both are spectral norms: given the

singular values $s_i(A) \geq 0$ of A , we may express these norms as

$$\|A\|_1 = \sum_i s_i(A), \quad \|A\|_{\infty} = \max_i s_i(A). \quad (18)$$

This induces corresponding operator norms for superoperators $\mathcal{M} : \mathfrak{gl}(\mathcal{H}^{\otimes t}) \rightarrow \mathfrak{gl}(\mathcal{H}^{\otimes t})$ by the usual

$$\|\mathcal{M}\|_p = \sup_{\substack{A \neq 0 \\ A \in \mathfrak{gl}(\mathcal{H}^{\otimes t})}} \frac{\|\mathcal{M}(A)\|_p}{\|A\|_p}. \quad (19)$$

We say \mathcal{E}_L forms a Gt -design if $\mathcal{A}_{\mathcal{E}_L}^{(t)} = 0$, and we say \mathcal{E}_L forms an ϵ -approximate Gt -design if $\|\mathcal{A}_{\mathcal{E}_L}^{(t)}\|_{\infty} \leq \epsilon$ for some $\epsilon > 0$. We prove the following theorem in the Supplemental Information:

Theorem 2. The ensemble of unitaries $\mathcal{E}_L \subseteq G$ generated by an L -layered circuit $U(\theta)$ will form an ϵ -approximate G 2-design, when the number of layers L is

$$L \geq \frac{\log(1/\epsilon)}{\log\left(1/\|\mathcal{A}_{\mathcal{E}_1}^{(2)}\|_{\infty}\right)}, \quad (20)$$

where \mathcal{E}_1 is the ensemble generated by a single layer $U_1(\theta_1)$.

We actually prove that this is true for any t , but to estimate the variance we need only $t=2$.

First, we note that Theorem 2 generalizes the result of¹⁷, which was only valid for problems where $\mathfrak{g} = \mathfrak{su}(2^n)$ or $\mathfrak{u}(2^n)$, to the case of an arbitrary DLA. Next, we can explicitly see that if the circuit is deep enough, i.e., if it has enough layers, it will always form an ϵ -approximate G 2-design, thus justifying the assumptions made in the main text. More concretely, if we know what the expressiveness for one layer is, Theorem 2 allows us to compute exactly how many layers are needed for $\|\mathcal{A}_{\mathcal{E}_L}^{(t)}\|_{\infty}$ to be smaller than a given ϵ . We present in the Supplemental Information an example where we can explicitly construct $\mathcal{A}_{\mathcal{E}_1}^{(2)}$ and obtain its largest eigenvalue. Finally, we note that the expressiveness of a single layer will depend on several choices in the ansatz such as how the gates are distributed in a single layer, and how the parameters are sampled therein. We leave the study of the single-layer expressiveness changes as a function of those factors for future work.

Variance for a circuit that does not form a 2-design over G

In the main text, we have assumed that the circuit is deep enough so that it forms a 2-design over G , and Theorem 2 provides bounds on the necessary number of layers for this to happen. Here, we instead ask the question: How different will the variance be from that in Theorem 1 if the circuit forms approximate, rather than an exact, 2-design over G ?

For this purpose, let us consider an L -layered circuit such as that in Eq. (1). In what follows, we do not assume that the circuit forms an approximate 2-design over G . Just as before, we denote the ensemble of unitaries generated by the L -layered circuit $U(\theta)$ by \mathcal{E}_L , and we define its t -th moment superoperator $\mathcal{M}_{\mathcal{E}_L}$ by Eq. (16). Then, denoting as $\text{Var}_{\mathcal{E}_L}$ and Var_G the variance obtained by sampling circuits over the distribution \mathcal{E}_L and over the Haar measure over G , respectively, we find that the following theorem holds.

Theorem 3. Let $\mathfrak{g} \subseteq \mathfrak{u}(2^n)$ be any dynamical Lie algebra, and suppose either ρ or O are in $i\mathfrak{g}$ with ρ a density matrix. Then the difference between the loss function variance of an L -layered circuit, with ensemble of unitaries \mathcal{E}_L , and the variance for a circuit that forms a

2-design over G can be bounded as

$$|\text{Var}_{\mathcal{E}_L}[\ell_{\theta}(\rho, O)] - \text{Var}_G[\ell_{\theta}(\rho, O)]| \leq 3 \left(\left\| \mathcal{A}_{\mathcal{E}_L}^{(2)} \right\|_{\infty} \right)^L \|O\|_F^2, \quad (21)$$

where the usual Schatten p -norm and induced Schatten p -norm are given by Eq. (18) and Eq. (19).

Theorem 3 shows that the variance of an L -layered circuit will converge exponentially fast in L to the variance obtained by assuming that $U(\theta)$ forms a 2-design. The rate of convergence is again determined by the single layers expressiveness $\left\| \mathcal{A}_{\mathcal{E}_1}^{(2)} \right\|_{\infty}$. As such, we can see that the assumption of U being a 2-design rapidly becomes an exact statement in the deep circuits regime. The proof of Theorem 3 is given in the Supplemental Information.

Variance as a sum over simple or abelian components

As noted in the main text, the DLA can always be decomposed into a direct sum as in Eq. (6). This implies that since G is compact, it must decompose as $G = G_1 \times \dots \times G_k$, with $G_j = e^{i\psi_j}$. Hence, any parametrized quantum circuit $U(\theta) \in G$ can be expressed as a tuple $U = (U_1, \dots, U_k)$, where we have omitted the dependence on θ for simplicity of notation. This realization allows us to show that the loss splits into a sum over the summands \mathfrak{g}_j in Eq. (6). Explicitly, for the case where $\mathfrak{g} = \mathfrak{g}_1 \oplus \mathfrak{g}_2$ with $O \in i\mathfrak{g}$ and $U(\theta) \in G$, we have

$$O = O_1 + O_2, \quad U(\theta) = (U_1, U_2),$$

where $O_j \in \mathfrak{g}_j$ and $U_j \in G_j$ for $j = 1, 2$. Hence, the loss function is

$$\ell_{\theta}(\rho, O) = \text{Tr}[\rho U(\theta)^\dagger O_1 U(\theta)] + \text{Tr}[\rho U(\theta)^\dagger O_2 U(\theta)].$$

Since $O_1 \in \mathfrak{g}_1$ commutes with any element of G_2 , we obtain

$$\begin{aligned} \text{Tr}[\rho U(\theta)^\dagger O_1 U(\theta)] &= \text{Tr}[\rho(U_1, U_2)^\dagger O_1(U_1, U_2)] \\ &= \text{Tr}[\rho(U_1, 1)^\dagger O_1(U_1, 1)] \\ &= : \ell_1(\rho, O_1). \end{aligned}$$

A similar result holds for the term $\text{Tr}[\rho U(\theta)^\dagger O_2 U(\theta)]$, and the loss function is expressible as a sum of losses in each simple or abelian component:

$$\ell_{\theta}(\rho, O) = \ell_1(\rho, O_1) + \ell_2(\rho, O_2). \quad (22)$$

Therefore, the mean value and the variance of $\ell_{\theta}(\rho, O)$ can also be expressed as the sum of individual terms in each simple or abelian component (additional details of the proof are provided in the Supplemental Information). This statement is formally captured as follows:

Proposition 1. Let O be in $i\mathfrak{g}$ such that $O = \sum_{i=1}^k O_i$ respect the decomposition Eq. (6) of \mathfrak{g} into simple and abelian components. Then, for any ρ , the expectation and variance of the loss function split into sums as

$$\begin{aligned} \mathbb{E}_{\theta}[\ell_{\theta}(\rho, O)] &= \sum_{i=1}^k \mathbb{E}_{G_i}[\ell_i(\rho, O_i)], \\ \text{Var}_{\theta}[\ell_{\theta}(\rho, O)] &= \sum_{i=1}^k \text{Var}_{G_i}[\ell_i(\rho, O_i)], \end{aligned} \quad (23)$$

where $\ell_i(\rho, O_i) = \text{Tr}[(1, \dots, U_i, \dots, 1)\rho(1, \dots, U_i, \dots, 1)^\dagger O_i]$ corresponds to the loss in the G_i -component of G .

We note that the previous result is equivalently valid if one exchanges the roles of O and ρ , that is, if $\rho \in i\mathfrak{g}$ and O is any Hermitian observable.

Special case: ρ or O simultaneously diagonalizable with a Cartan subalgebra

Here, we focus on the case where one chooses a Cartan subalgebra $\mathfrak{h} \subset \mathfrak{g}$ and ρ (or O) is simultaneously diagonalizable with \mathfrak{h} , i.e., $[\rho, \mathfrak{h}] = 0$. A basis of \mathcal{H} diagonalizing \mathfrak{h} is called a weight basis, and when ρ is diagonalized by this basis, the \mathfrak{g} -purity is straightforward to compute. We first demonstrate this situation by revisiting a calculation from ref. 17, which concerns the case where $\mathfrak{g} = \mathfrak{su}(2)$ is irreducibly represented in \mathcal{H} . We then generalize this calculation to an arbitrary simple DLA \mathfrak{g} .

Let \mathfrak{g} be the irreducible spin- S representation of $\mathfrak{su}(2)$ acting on $\mathcal{H} = \mathbb{C}^{2S+1}$. We have a basis for $i\mathfrak{g}$ given by the usual Hermitian spin matrices $\{S_x, S_y, S_z\} \subseteq \mathfrak{gl}(\mathcal{H})$. One can pick the Cartan subalgebra $i\mathfrak{h} = \text{span}_{\mathbb{R}}(S_z)$. A convenient orthonormal basis for \mathcal{H} is then given by $\{|m\rangle\}$, the eigenvectors of S_z , which satisfy

$$S_z|m\rangle = m|m\rangle, \quad m = -S, -S+1, \dots, S-1, S. \quad (24)$$

Let us consider the case where $\rho = |m\rangle\langle m|$ and $O \in i\mathfrak{g}$. To use Theorem 1, we will need to compute $\rho_{\mathfrak{g}}$. Such projection can be easily computed by performing a change of basis of $\mathfrak{g}_{\mathbb{C}} = \text{span}_{\mathbb{C}}\mathfrak{g}$ from the spin matrices to $\{S_0, S_+, S_-\}$, where

$$S_0 = \frac{1}{\sqrt{c_z}} S_z, \quad S_+ = \frac{1}{\sqrt{c_+}} (S_x + iS_y), \quad S_- = \frac{1}{\sqrt{c_-}} (S_x - iS_y),$$

with the c 's being normalization constants such that $\text{Tr}[S_0^2] = 1$ and $\text{Tr}[S_+^\dagger S_+] = \text{Tr}[S_-^\dagger S_-] = 1$ (in particular we find that $c_z = \text{Tr}[S_z^2] = \frac{1}{2}S(S+1)(2S+1)$). On the basis $\{|m\rangle\}$ of \mathcal{H} , S_z is diagonal, S_+ is upper triangular nilpotent, and S_- is lower triangular nilpotent. A direct calculation shows that $\text{Tr}[S_+^\dagger \rho] = \text{Tr}[S_-^\dagger \rho] = 0$, and thus

$$\rho_{\mathfrak{g}} = \rho_{\mathfrak{h}} = \frac{1}{c_z} \text{Tr}[S_z \rho] S_z = \frac{m}{c_z} S_z. \quad (25)$$

Then, replacing Eq. (25) into Theorem 1 and using $\dim(\mathfrak{g}) = 3$ leads to

$$\text{Var}_{\theta}[\ell_{\theta}(\rho, O)] = \frac{m^2 \text{Tr}[O^2]}{S(S+1)(2S+1)}. \quad (26)$$

Note that $S(S+1)$ is exactly the action of the Casimir element on \mathcal{H} . For the case of $O = S_z/S$ (where we normalized the measurement operator so that $\|O\| = 1$), we find that Eq. (26) becomes $\text{Var}_{\theta}[\ell_{\theta}(\rho, O)] = \frac{m^2}{3S^2}$. Hence, we can see that the loss function concentrates depending on the value m , i.e., on the \mathfrak{g} -purity or the generalized entanglement present in the initial state.

The previous example can be used as a starting point to calculate the loss variance for ρ being a sum of weight states. In particular, consider the case where \mathfrak{g} is simple. We can always find an orthonormal basis of weight spaces for \mathcal{H} by simultaneously diagonalizing a Cartan subalgebra \mathfrak{h} of \mathfrak{g} . This means that we have an orthonormal basis $\{|\nu\rangle\}$ for \mathcal{H} , so that $|\nu\rangle$ has weight λ_{ν} , i.e.

$$H_j |\nu\rangle = \lambda_{\nu}(H_j) |\nu\rangle, \quad \text{for all } H_j \in i\mathfrak{h}. \quad (27)$$

Note that the eigenvalues $\lambda_{\nu}(H_j)$ are real as H_j are Hermitian. Then a pure weight state with respect to \mathfrak{h} has the form $\rho = |\nu\rangle\langle\nu|$. We say that ρ is a weight state if it is diagonal with respect to the weight basis, i.e., if

$$\rho = \sum_{\nu} r_{\nu} |\nu\rangle\langle\nu|, \quad r_{\nu} \geq 0, \quad \sum_{\nu} r_{\nu} = 1. \quad (28)$$

As shown in the Supplemental Information, given an orthonormal basis $\{H_j\}_{j=1}^{\dim(\mathfrak{h})}$ of $i\mathfrak{h}$, one can find that

$$\rho_{\mathfrak{g}} = \rho_{\mathfrak{h}} = \sum_{j=1}^{\dim(\mathfrak{h})} \lambda_{\rho}(H_j) H_j, \quad \text{with } \lambda_{\rho} = \sum_v r_v \lambda_v. \quad (29)$$

Hence,

$$\text{Tr}[\rho_{\mathfrak{g}}^2] = \sum_{j=1}^{\dim(\mathfrak{h})} \lambda_{\rho}(H_j)^2 = \|\lambda_{\rho}\|^2. \quad (30)$$

Then, plugging into Theorem 1 yields the following corollary.

Corollary 2. Let \mathfrak{g} be a simple Lie algebra with a Cartan subalgebra \mathfrak{h} . Let $O \in ig$, and ρ be a density matrix with $[\rho, \mathfrak{h}] = 0$, that is, a weight state as in Eq. (28). Then the variance of the loss function is given by

$$\text{Var}_{\theta}[\ell_{\theta}(\rho, O)] = \frac{\text{Tr}[O^2]}{\dim(\mathfrak{g})} \|\lambda_{\rho}\|^2. \quad (31)$$

Here, we find it important to make three remarks. First, by symmetry, the result of Corollary 2 also holds when the roles of ρ and O are reversed, i.e., when $\rho \in ig$ and $[O, \mathfrak{h}] = 0$. Second, the variance does not depend on the choice of Cartan subalgebra, only on the norm of the weight λ_{ρ} corresponding to the weight state ρ , because all Cartan subalgebras are conjugate to each other. Finally, we note that among all weights λ_v in an irreducible representation \mathcal{H} , the norm $\|\lambda_v\|$ is maximized when $|v\rangle$ is the highest weight vector $|hw\rangle$. Thus, Eq. (31) implies that among all weight states as in Eq. (28), the variance is maximized when ρ is a highest weight state:

$$\arg \max_{\rho \text{ as in Eq.(28)}} \text{Var}_{\theta}[\ell_{\theta}(\rho, O)] = |hw\rangle \langle hw|. \quad (32)$$

From here, we can derive an estimate for the variance as follows. Consider the bilinear form on \mathfrak{g} given by $(A, B) = \text{Tr}_{\mathbb{C}^N}[AB]$ where the trace is taken over the defining representation \mathbb{C}^N of $\mathfrak{g} = \mathfrak{su}(N)$, $\mathfrak{so}(N)$ or $\mathfrak{sp}(N)$; this is the standard bilinear form normalized so that $(H, H) = 2$ or 4 for simple coroots $H \in i\mathfrak{h}$ (for $\mathfrak{g} = \mathfrak{su}(N)$, these are the diagonal matrices with $0, \dots, 0, 1, -1, 0, \dots, 0$ on the diagonal). The highest weight λ_{hw} of every irreducible finite-dimensional representation \mathcal{H} of \mathfrak{g} has the property that $\lambda_{hw}(H)$ is a non-negative integer for any simple coroot H . We assume that these values will not grow with the system size n . Noting that $(A, B) = \frac{\dim(\mathcal{H})}{N} (A, B)$ for Hermitian operators $A, B \in ig$, we see that the basis vectors H_j of $i\mathfrak{h}$ scale as $\sqrt{N/2^n}$ times the simple coroots of $i\mathfrak{h}$. Therefore,

$$\|\lambda_{hw}\|^2 \in \Theta\left(\frac{N}{2^n}\right) = \Theta\left(\frac{\sqrt{\dim(\mathfrak{g})}}{2^n}\right). \quad (33)$$

Plugging this in Eq. (31), we obtain the upper bound

$$\text{Var}_{\theta}[\ell_{\theta}(\rho, O)] \in \mathcal{O}\left(\frac{\text{Tr}[O^2]}{2^n \sqrt{\dim(\mathfrak{g})}}\right). \quad (34)$$

Hence, we see that if $\text{Tr}[O^2] \leq 2^n$ and $\dim(\mathfrak{g}) \in \Omega(b^n)$ with $b > 1$, then $\text{Var}_{\theta}[\ell_{\theta}(\rho, O)] \in \mathcal{O}(\frac{1}{\sqrt{b^n}})$; indicating that if the DLA is simple and of exponential dimension, then the loss will always have a BP regardless of the measurement operator and initial state.

Reporting summary

Further information on research design is available in the Nature Portfolio Reporting Summary linked to this article.

Data availability

Data generated and analyzed during the current study are available from the corresponding author upon reasonable request.

References

- Cerezo, M. et al. Variational quantum algorithms. *Nat. Rev. Phys.* **3**, 625–644 (2021).
- Bharti, K. et al. Noisy intermediate-scale quantum algorithms. *Rev. Mod. Phys.* **94**, 015004 (2022).
- Endo, S., Cai, Z., Benjamin, S. C. & Yuan, X. Hybrid quantum-classical algorithms and quantum error mitigation. *J. Phys. Soc. Jpn* **90**, 032001 (2021).
- Peruzzo, A. et al. A variational eigenvalue solver on a photonic quantum processor. *Nat. Commun.* **5**, 1 (2014).
- Farhi, E., Goldstone, J., & Gutmann, S. A quantum approximate optimization algorithm. Preprint at arXiv <https://doi.org/10.48550/arXiv.1411.4028> (2014).
- Hadfield, S. et al. From the quantum approximate optimization algorithm to a quantum alternating operator ansatz. *Algorithms* **12**, 34 (2019).
- Schuld, M., Sinayskiy, I. & Petruccione, F. An introduction to quantum machine learning. *Contemp. Phys.* **56**, 172 (2015).
- Biamonte, J. et al. Quantum machine learning. *Nature* **549**, 195 (2017).
- Benedetti, M., Lloyd, E., Sack, S. & Fiorentini, M. Parameterized quantum circuits as machine learning models. *Quantum Sci. Technol.* **4**, 043001 (2019).
- Havlíček, V. et al. Supervised learning with quantum-enhanced feature spaces. *Nature* **567**, 209 (2019).
- Anschuetz, E. R. & Kiani, B. T. Beyond barren plateaus: Quantum variational algorithms are swamped with traps. *Nat. Commun.* **13**, 7760 (2022).
- Bittel, L. & Kliesch, M. Training variational quantum algorithms is NP-hard. *Phys. Rev. Lett.* **127**, 120502 (2021).
- McClean, J. R., Boixo, S., Smelyanskiy, V. N., Babbush, R. & Neven, H. Barren plateaus in quantum neural network training landscapes. *Nat. Commun.* **9**, 1 (2018).
- Holmes, Z., Sharma, K., Cerezo, M. & Coles, P. J. Connecting ansatz expressibility to gradient magnitudes and barren plateaus. *PRX Quantum* **3**, 010313 (2022).
- Marrero, C. O., Kieferová, M. & Wiebe, N. Entanglement-induced barren plateaus. *PRX Quantum* **2**, 040316 (2021).
- Patti, T. L., Najafi, K., Gao, X. & Yelin, S. F. Entanglement devised barren plateau mitigation. *Phys. Rev. Res.* **3**, 033090 (2021).
- Larocca, M. et al. Diagnosing barren plateaus with tools from quantum optimal control. *Quantum* **6**, 824 (2022).
- Friedrich, L. & Maziero, J. Quantum neural network cost function concentration dependency on the parametrization expressivity. *Sci. Rep.* **13**, 9978 (2023).
- Sharma, K., Cerezo, M., Cincio, L. & Coles, P. J. Trainability of dissipative perceptron-based quantum neural networks. *Phys. Rev. Lett.* **128**, 180505 (2022).
- Kieferova, M., Carlos, O. M., & Wiebe, N. Quantum generative training using rényi divergences. Preprint at arXiv <https://doi.org/10.48550/arXiv.2106.09567> (2021).
- Pesah, A. et al. Absence of barren plateaus in quantum convolutional neural networks. *Phys. Rev. X* **11**, 041011 (2021).
- Lee, J., Magann, A. B., Rabitz, H. A. & Arenz, C. Progress toward favorable landscapes in quantum combinatorial optimization. *Phys. Rev. A* **104**, 032401 (2021).

23. Martín, E. C., Plekhanov, K. & Lubasch, M. Barren plateaus in quantum tensor network optimization. *Quantum* **7**, 974 (2023).
24. Grimsley, H. R., Mayhall, N. J., Barron, G. S., Barnes, E. & Economou, S. E. Adaptive, problem-tailored variational quantum eigensolver mitigates rough parameter landscapes and barren plateaus. *NPJ Quantum Info.* **9**, 19 (2023).
25. Sack, S. H., Medina, R. A., Michailidis, A. A., Kueng, R. & Serbyn, M. Avoiding barren plateaus using classical shadows. *PRX Quantum* **3**, 020365 (2022).
26. Cerezo, M., Sone, A., Volkoff, T., Cincio, L. & Coles, P. J. Cost function dependent barren plateaus in shallow parametrized quantum circuits. *Nat. Commun.* **12**, 1 (2021).
27. Uvarov, A. & Biamonte, J. D. On barren plateaus and cost function locality in variational quantum algorithms. *J. Phys A Math. Theor.* **54**, 245301 (2021).
28. Kashif, M. & Al-Kuwari, S. The impact of cost function globality and locality in hybrid quantum neural networks on nisq devices. *Mach. Learn. Sci. Technol.* **4**, 015004 (2023).
29. Khatri, S. et al. Quantum-assisted quantum compiling. *Quantum* **3**, 140 (2019).
30. Uvarov, A., Biamonte, J. D. & Yudin, D. Variational quantum eigensolver for frustrated quantum systems. *Phys. Rev. B* **102**, 075104 (2020).
31. Leadbeater, C., Sharrock, L., Coyle, B. & Benedetti, M. F-divergences and cost function locality in generative modelling with quantum circuits. *Entropy* **23**, 1281 (2021).
32. Cerezo, M., Sharma, K., Arrasmith, A. & Coles, P. J. Variational quantum state eigensolver. *NPJ Quantum Info.* **8**, 1 (2022).
33. Thanaslip, S., Wang, S., Nghiem, N. A., Coles, P. J. & Cerezo, M. Subtleties in the trainability of quantum machine learning models. *Quantum Mach. Intell.* **5**, 21 (2023).
34. Shaydulin, R. & Wild, S. M. Importance of kernel bandwidth in quantum machine learning. *Phys. Rev. A* **106**, 042407 (2022).
35. Abbas, A. et al. The power of quantum neural networks. *Nat. Comput. Sci.* **1**, 403 (2021).
36. Leone, L., Oliviero, S. F. E., Cincio, L. & Cerezo, M. On the practical usefulness of the hardware efficient ansatz. *Quantum* **8**, 1395 (2024).
37. Holmes, Z. et al. Barren plateaus preclude learning scramblers. *Phys. Rev. Lett.* **126**, 190501 (2021).
38. Wang, S. et al. Noise-induced barren plateaus in variational quantum algorithms. *Nat. Commun.* **12**, 1 (2021).
39. Stilck França, D. & Garcia-Patron, R. Limitations of optimization algorithms on noisy quantum devices. *Nat. Phys.* **17**, 1221 (2021).
40. García-Martín, D., Larocca, M. & Cerezo, M. Effects of noise on the overparametrization of quantum neural networks. *Phys. Rev. Research* **6**, 013295 (2024).
41. Arrasmith, A., Holmes, Z., Cerezo, M. & Coles, P. J. Equivalence of quantum barren plateaus to cost concentration and narrow gorges. *Quantum Sci. Technol.* **7**, 045015 (2022).
42. Zeier, R. & Schulte-Herbrüggen, T. Symmetry principles in quantum systems theory. *J. Math. Phys.* **52**, 113510 (2011).
43. D'Alessandro D. *Introduction to Quantum Control and Dynamics* Chapman & Hall/CRC Applied Mathematics & Nonlinear Science (Taylor & Francis, 2007).
44. Zimborás, Z., Zeier, R., Schulte-Herbrüggen, T. & Burgarth, D. Symmetry criteria for quantum simulability of effective interactions. *Phys. Rev. A* **92**, 042309 (2015).
45. Knapp A. W. *Lie Groups Beyond an Introduction* Vol. 140 (Springer Science & Business Media, 2013).
46. Dankert, C., Cleve, R., Emerson, J. & Livine, E. Exact and approximate unitary 2-designs and their application to fidelity estimation. *Phys. Rev. A* **80**, 012304 (2009).
47. Collins, B., Matsumoto, S. & Novak, J. The weingarten calculus. *Amer. Math. Soc.* **69**, 734 (2022).
48. Somma, R., Ortiz, G., Barnum, H., Knill, E. & Viola, L. Nature and measure of entanglement in quantum phase transitions. *Phys. Rev. A* **70**, 042311 (2004).
49. Somma, R. D. Quantum computation, complexity, and many-body physics. Preprint at <https://doi.org/10.48550/arXiv.quant-ph/0512209> (2005).
50. Kökcü, E. et al. Fixed depth hamiltonian simulation via cartan decomposition. *Phys. Rev. Lett.* **129**, 070501 (2022).
51. Schatzki, L., Larocca, M., Nguyen, Q. T., Sauvage, F. & Cerezo, M. Theoretical guarantees for permutation-equivariant quantum neural networks. *npj Quantum Information* **10**, 12 (2024).
52. Kazi, S., Larocca, M. & Cerezo, M. On the universality of s_n -equivariant k -body gates. *New Journal of Physics* **26**, 053030 (2024).
53. Wiersema, R., Kökcü, E., Kemper, A. F. & Bakalov, B. N. Classification of dynamical Lie algebras of 2-local spin systems on linear, circular and fully connected topologies. Preprint at arXiv <https://doi.org/10.48550/arXiv.2309.05690> (2023).
54. Barnum, H., Knill, E., Ortiz, G. & Viola, L. Generalizations of entanglement based on coherent states and convex sets. *Phys. Rev. A* **68**, 032308 (2003).
55. Barnum, H., Knill, E., Ortiz, G., Somma, R. & Viola, L. A subsystem-independent generalization of entanglement. *Phys. Rev. Lett.* **92**, 107902 (2004).
56. Diaz, N. L., García-Martín, D., Kazi, S., Larocca, M. & Cerezo, M. Showcasing a barren plateau theory beyond the dynamical lie algebra. Preprint at arXiv <https://doi.org/10.48550/arXiv.2310.11505> (2023).
57. Heyraud, V., Li, Z., Donatella, K., Boité, A. L. & Ciuti, C. Efficient estimation of trainability for variational quantum circuits. *PRX Quantum* **4**, 040335 (2023).
58. Liu, Z., Yu, L.-W., Duan, L.-M. & Deng, D.-L. The presence and absence of barren plateaus in tensor-network based machine learning. *Phys. Rev. Lett.* **129**, 270501 (2022).
59. Barthel, T., & Miao, Q. Absence of barren plateaus and scaling of gradients in the energy optimization of isometric tensor network states. Preprint at arXiv <https://doi.org/10.48550/arXiv.2304.00161> (2023).
60. Miao, Q. & Barthel, T. Isometric tensor network optimization for extensive hamiltonians is free of barren plateaus. *Phys. Rev. A* **109**, L050402 (2024).
61. Garcia, R. J., Zhao, C., Bu, K. & Jaffe, A. Barren plateaus from learning scramblers with local cost functions. *J. High Energy Phys.* **2023**, 1 (2023).
62. Letcher, A., Woerner, S. & Zoufal, C. From tight gradient bounds for parameterized quantum circuits to the absence of barren plateaus in qgans. Preprint at arXiv <https://doi.org/10.48550/arXiv.2309.12681> (2023).
63. Arrazola, J. M. et al. Universal quantum circuits for quantum chemistry. *Quantum* **6**, 742 (2022).
64. Zhang, H.-K., Liu, S. & Zhang, S.-X. Absence of barren plateaus in finite local-depth circuits with long-range entanglement. *Phys. Rev. Lett.* **132**, 150603 (2024).
65. Napp, J. Quantifying the barren plateau phenomenon for a model of unstructured variational ansätze. Preprint at arXiv <https://doi.org/10.48550/arXiv.2203.06174> (2022).
66. Braccia, P., Bermejo, P., Cincio, L. & Cerezo, M. Computing exact moments of local random quantum circuits via tensor networks. Preprint at arXiv <https://doi.org/10.48550/arXiv.2403.01706> (2024).
67. Hu H.-Y. et al. Demonstration of robust and efficient quantum property learning with shallow shadows. Preprint at arXiv <https://doi.org/10.48550/arXiv.2402.17911> (2024).
68. Zhao, C. & Gao, X.-S. Analyzing the barren plateau phenomenon in training quantum neural networks with the ZX-calculus. *Quantum* **5**, 466 (2021).

69. Cerezo M. et al. Does provable absence of barren plateaus imply classical simulability? or, why we need to rethink variational quantum computing. Preprint at arXiv <https://doi.org/10.48550/arXiv.2312.09121> (2023).
70. Larocca, M., Ju, N., García-Martín, D., Coles, P. J. & Cerezo, M. Theory of overparametrization in quantum neural networks. *Nat. Comput. Sci.* **3**, 542 (2023).
71. Marvian, I. Restrictions on realizable unitary operations imposed by symmetry and locality. *Nat. Phys.* **18**, 283 (2022).
72. Fontana E. et al. Characterizing barren plateaus in quantum ansätze with the adjoint representation. *Nat. Commun.* <https://doi.org/10.1038/s41467-024-49910-w> (2024).
73. Marvian, I. (Non-)universality in symmetric quantum circuits: Why abelian symmetries are special. Preprint at arXiv <https://doi.org/10.48550/arXiv.2302.12466> (2023).

Acknowledgements

We thank Zoe Holmes, Mark Wilde, and Akram Touil for fruitful discussions about superoperator norms. We are extremely grateful to Lukasz Cincio for his help with numerical calculations. M.R. and C.O.M. were supported by the Laboratory Directed Research and Development Program and Mathematics for Artificial Reasoning for Scientific Discovery investment at the Pacific Northwest National Laboratory, a multiprogram national laboratory operated by Battelle for the U.S. Department of Energy under Contract DE-AC05-76RLO1830. B.N.B. was supported in part by a Simons Foundation grant No. 584741. F.S. and M.C. acknowledge support by the Laboratory Directed Research and Development program of Los Alamos National Laboratory (LANL) under project numbers 20230049DR and 20230527ECR. A.F.K. was supported in part by the National Science Foundation under award No. 1818914: PFCQC: STAQ: Software-Tailored Architecture for Quantum co-design and No. 2325080: Software-Tailored Architecture for Quantum Co-Design (STAQ). M.L. was supported by the Center for Nonlinear Studies at LANL. M.C. was initially supported by LANL ASC Beyond Moore's Law project.

Author contributions

The project was conceived by B.N.B., C.O.M., M.L., and M.C. Theoretical results were derived by B.N.B., M.R., and M.C., with some independently verified by M.L. and M.C. Numerical simulations were performed by F.S.

and M.C. The manuscript was mainly written by M.C., M.R., B.N.B., and A.F.K. All authors contributed to the manuscript review process.

Competing interests

The authors declare no competing interests.

Additional information

Supplementary information The online version contains supplementary material available at <https://doi.org/10.1038/s41467-024-49909-3>.

Correspondence and requests for materials should be addressed to M. Cerezo.

Peer review information *Nature Communications* thanks the anonymous reviewer(s) for their contribution to the peer review of this work. A peer review file is available.

Reprints and permissions information is available at <http://www.nature.com/reprints>

Publisher's note Springer Nature remains neutral with regard to jurisdictional claims in published maps and institutional affiliations.

Open Access This article is licensed under a Creative Commons Attribution-NonCommercial-NoDerivatives 4.0 International License, which permits any non-commercial use, sharing, distribution and reproduction in any medium or format, as long as you give appropriate credit to the original author(s) and the source, provide a link to the Creative Commons licence, and indicate if you modified the licensed material. You do not have permission under this licence to share adapted material derived from this article or parts of it. The images or other third party material in this article are included in the article's Creative Commons licence, unless indicated otherwise in a credit line to the material. If material is not included in the article's Creative Commons licence and your intended use is not permitted by statutory regulation or exceeds the permitted use, you will need to obtain permission directly from the copyright holder. To view a copy of this licence, visit <http://creativecommons.org/licenses/by-nc-nd/4.0/>.

© The Author(s) 2024